Amplified mid-latitude planetary waves favour particular regional weather extremes

James A. Screen[1] & Ian Simmonds[2]

[1]*College of Engineering, Mathematics and Physical Sciences, University of Exeter, Exeter EX4 4QF, UK.*

[2]*School of Earth Sciences, The University of Melbourne, Melbourne, Victoria 3010, Australia.*

There has been an ostensibly large number of extreme weather events in the northern hemisphere mid-latitudes during the last decade[1]. An open question that is critically important for scientists and policy makers is whether any such increase in weather extremes is natural or anthropogenic in origin[2-14]. One mechanism proposed to explain the increased frequency of extreme weather events is the amplification of mid-latitude atmospheric planetary waves[15-17]. Disproportionately large warming in the northern polar regions compared to mid-latitudes – and associated weakening of the north-south temperature gradient - may favour larger amplitude planetary waves[15,17], although observational evidence for this remains inconclusive[18-20]. A better understanding of the role of planetary waves in causing mid-latitude weather extremes is essential for assessing the potential environmental and socio-economic impacts of future planetary wave changes. Here we show that months of extreme weather over mid-latitudes are commonly accompanied by

significantly amplified quasi-stationary mid-tropospheric planetary waves, with zonal wave numbers of 3-8. Conversely, months of near-average weather over mid-latitudes are often accompanied by significantly attenuated wave numbers 3-8. Depending on geographical region, certain types of extreme weather (e.g., hot, cold, wet, dry) are more strongly related to wave amplitude changes than others. The findings suggest that amplification of quasi-stationary wave numbers 3-8 preferentially increases the probabilities of heat waves in western North America and central Asia, cold outbreaks in eastern North America, droughts in central North America, Europe and central Asia, and wet spells in western Asia.

A series of weather extremes have hit the Northern Hemisphere mid-latitudes in the recent years[1], such as the European heat wave in summer 2003[8], cold and snowy winters in 2009/10, 2010/11 and 2013/14 in northeast United States[16], the Russian heat wave in summer 2010[2-5], Texas drought of 2011[6], and the summer 2012 and winter 2013/14 floods in United Kingdom[7]; all have had significant socio-economic impacts. There is increasing scientific evidence[1-14] and a growing public perception[21] that extreme weather events are occurring more frequently. However, the mechanisms that drive weather extremes and through which climate change may influence climate variability are poorly understood. A potential cause of increased weather extremes is the amplification of atmospheric planetary waves[15-17]. Empirical[15,16], dynamical[17] and modelling[16,22] evidence suggest a weakening north-south temperature gradient – a key characteristic of anthropogenic climate change[23,24] – causes larger amplitude planetary waves, and it is hypothesised that high-amplitude planetary

50 waves favour the occurrence of extreme weather. It is this hypothesis that we

51 examine here.

52

53 First, it is necessary to define precisely "extreme weather" for this application.

54 We are concerned with persistent anomalies in land surface temperature (T_L)

55 and land precipitation (P_L), such as heat waves, cold spells, droughts and

56 prolonged wet periods, which are evident on monthly timescales and large

57 spatial scales (see Methods). Initially we focus on absolute (i.e., irrespective of

58 their sign) T_L and P_L anomalies (denoted $|T_L'|$ and $|P_L'|$). This is appropriate

59 because planetary waves tend to induce positive T_L (and perhaps P_L) anomalies

60 at some longitudes and negative anomalies at other longitudes.

61

62 Fig. 1a,b show normalized time-series for monthly $|T_L'|$ and $|P_L'|$, respectively,

63 area-averaged over northern mid-latitudes (35-60°N; ML). The 40 months with

64 largest values (approx. 10% of cases) are highlighted by circles and labelled on

65 the lower x-axis. The months of extreme T_L and P_L lie relatively evenly through

66 the 34-year period, and there is no long-term trend. A full discussion of 34-year

67 trends in $|T_L'|$ and $|P_L'|$ is provided in the Supplementary Discussion S1. Fig. 1c

68 shows planetary-wave amplitude anomalies (normalized by removing the mean

69 amplitude and dividing by the standard deviation, σ, for each wave number) for

70 wave numbers 3-8 during months of T_L extremes (i.e., the months shown by

71 circles in Fig. 1a). The overwhelming majority of the statistically significant

72 amplitude anomalies are positive. The number of significant positive anomalies

73 (32) is appreciably larger than would be expected by chance alone (12). On half

74 of the extreme months considered there is at least one significant positive

75   amplitude anomaly for wave numbers 3-8. The three months with significant

76   negative amplitude anomalies also have at least one significant positive

77   amplitude anomaly. Thus, it would appear that some wave numbers are

78   amplified at the expense of other wave numbers. Although significantly amplified

79   planetary-waves are common during months of T_L extremes, it is not always the

80   same wave number(s) that is/are amplified. The greatest number of significant

81   positive amplitude anomalies are found for wave numbers 5, 6 and 7. Positive

82   monthly-mean amplitude anomalies imply, in physical terms, highly meridional

83   and persistent (slow-moving) circulation regimes (see Supplementary

84   Discussion S2).

85

86   The statistically significant planetary-wave amplitude anomalies during months

87   of P_L extremes (i.e., the months shown by circles in Fig. 1b) are also

88   predominantly positive (Fig. 1d). Significantly amplified waves, in at least one

89   wave number 3-8, are identified in 40% of the months with extreme P_L. This

90   percentage increases to 50% for the 20 months with most extreme P_L. In

91   contrast, only one of these 20 months displays a significant negative amplitude

92   anomaly and further, this is accompanied by positive anomalies in two other

93   wave numbers. As for T_L, this suggests a link between extreme P_L and

94   significantly amplified planetary waves. However, clearly not all months with T_L

95   or P_L extremes are associated with significantly amplified, or attenuated,

96   planetary-wave amplitudes.

97

98   Fig. 2a shows the probability density function (PDF) of amplitude anomalies for

99   each of wave numbers 3-8 in each of the 40 months of T_L extremes. Months of T_L

100 extremes over ML are associated with significantly amplified planetary waves, in

101 the sense that positive amplitude anomalies occur relatively more often during

102 months of T_L extremes than they do climatologically. The difference in mean

103 amplitude anomalies, between extreme months and climatology, is very highly

104 statistically significant ($p < 0.001$). The difference in amplitude variance is also

105 highly significant ($p < 0.01$), with greater variance in months of T_L extremes than

106 climatologically. This increase in variance is primarily due to larger frequencies

107 at the positive tail of the distribution. This suggests that not only are T_L extremes

108 associated with amplified waves on average, but also that there is an particularly

109 strong association between the most highly amplified planetary waves and

110 extreme T_L.

111

112 On the basis of daily reanalysis data, it can be seen that planetary-wave

113 amplitude and $|T_L'|$ co-vary almost simultaneously, but with the temperature

114 anomalies lagging the amplitude anomalies by 1-2 days (Supplementary Figure

115 3). This time lag implies that surface temperatures are responding to the

116 atmospheric circulation anomalies and not the other way round. Furthermore,

117 whilst surface temperatures respond very rapidly to circulation changes (hours

118 to days), the timescale for the mid-tropospheric circulation (wave amplitude is

119 defined at 500 hPa; see Methods) to respond to surface temperature anomalies is

120 much slower (tens of days to months). Thus irrespective of the small time lag, the

121 timescale of the response is strongly suggestive of a causal link between

122 planetary-wave amplitude and temperature extremes (see Supplementary

123 Discussion S3).

124

125 Fig. 2b-h show PDFs for the planetary-wave amplitude anomalies during months

126 with T_L extremes over seven geographical regions (shown in Fig. 3). Over wNAm,

127 cNAm and Euro, T_L extremes are associated with significantly larger mean

128 amplitude and greater amplitude variance, consistent with the results for ML. T_L

129 extremes over eNAm are linked to increased amplitude variance, but not

130 significantly different mean amplitude. Over eAsia, significantly attenuated

131 planetary-wave amplitudes accompany T_L extremes.

132

133 Analogous PDFs for months of P_L extremes are shown in Fig. 2i-p. As for T_L

134 extremes, we find that P_L extremes over ML are associated with significantly

135 larger mean amplitude and significantly larger variance (again, the latter is

136 primarily due to greater frequencies at the positive tail of the PDF). Regional P_L

137 extremes over wNAm, Euro and wAsia are also linked to significantly amplified

138 waves.

139

140 The association between planetary-wave amplitude and mid-latitude- mean $|T_L'|$

141 exists over a wide range of timescales from daily to sub-seasonal. The strength of

142 this relationship is relatively insensitive to timescale, although is it marginally

143 strongest on 5-14 day timescales (Supplementary Discussion S5). In contrast, the

144 amplitude-precipitation relationship weakens for timescales less than 12 days.

145 This implies that planetary waves are more important for longer-duration

146 precipitation extremes, such as those that contribute to drought, than they are

147 for short-lived precipitation extremes. We speculate that precipitation variability

148 is closely related to synoptic- or local-scale drivers on short timescales whereas

149   longer-lived events are more closely tied to the large-scale atmospheric
150   circulation.

151

152   If extreme weather is linked to amplified waves, is near-average weather
153   accompanied by attenuated planetary waves? Months of near-average (see
154   Methods for definition) T_L over ML and wNAm are associated with, on average,
155   significantly attenuated planetary-wave amplitudes, whereas months of near-
156   average T_L over eAsia are accompanied by significantly amplified waves (Fig. 3).
157   All these relationships are opposite to those found for months with extreme T_L.
158   In Euro and wAsia, amplitude variance is significantly lower in months of
159   extreme T_L than climatologically. From the PDFs, it can be seen that this
160   primarily reflects fewer cases of large positive amplitude anomalies during the
161   months of near-average T_L than climatologically. Whilst months with T_L extremes
162   are often accompanied by highly amplified waves, these rarely accompany
163   months with near-average T_L. Turning to precipitation, none of the geographical
164   regions show a significant difference in mean amplitude anomaly between
165   months of near-average P_L and climatology (Fig. 3i-p). However, amplitude
166   variance is significantly lower over ML and wNAm, as a consequence of fewer (in
167   percentage terms) large positive amplitude anomalies during months of near-
168   average P_L than in all months taken together.

169

170   It is reasonable to expect that any particular planetary wave will induce positive
171   T_L (and perhaps P_L) anomalies at some longitudes and negative anomalies at
172   other longitudes. If wave phase was highly variable in time (i.e., the waves were
173   "free"), amplified waves might favour extremes of both sign (hot or cold, wet or

174   dry) at any specific longitude. However in reality, the waves have preferred

175   phases (i.e., they are quasi-stationary), related to orography and climatological-

176   mean thermal gradients[15,25]. This is especially the case for the smaller wave

177   numbers. Further, at any particular location, T_L and P_L may be more sensitive to

178   amplitude anomalies of one sign than the other, or to some wave numbers and

179   phases than others. Therefore, amplified waves may in fact favour one type of

180   extreme weather more than another, in any specific location. Table 1 compares

181   the mean amplitude and variance in regionally hot, cold, wet and dry months to

182   climatological mean amplitude and variance (the full PDFs are shown in

183   Supplementary Discussion S5). Consistent with the rationale above, it appears

184   that in most regions there are stronger links between planetary-wave amplitude

185   and weather extremes of one sign than extremes of the other. Significantly

186   amplified waves are found during hot extremes over wNAm and cAsia, cold

187   extremes over eNAm, dry extremes over Euro and cAsia, and wet extremes over

188   wAsia. In each case, extremes of opposite sign in the same region are not

189   accompanied by significantly amplified, or attenuated, planetary waves.

190   Precipitation extremes over cNAm are an interesting case: amplified waves tend

191   to accompany dry extremes whereas attenuated waves preferentially occur

192   during wet extremes.

193

194   These findings reinforce suggestions that amplified planetary waves favour

195   extreme weather in mid-latitudes[15-17,26]. However, previous studies have not

196   determined which types of extreme weather are caused by amplified waves, or

197   where these extremes are likely to occur. Clearly these details are critically

198   important for decision makers in assessing the risk of, and planning for the

199 impacts of, extreme weather events in the future. If quasi-stationary wave

200 numbers 3-8 are amplified in response to anthropogenic climate change, as has

201 been proposed[15,17], our results suggest that this would preferentially increase the

202 probabilities of heat waves in western North America and central Asia, cold

203 waves in eastern North America, droughts in central North America, Europe and

204 central Asia, and wet extremes in western Asia. However, robust observational

205 evidence for long-term trends in planetary-wave amplitude is lacking[18-20] and

206 further work is required to understand better the physical mechanisms through

207 which human-induced climate change may impact upon mid-latitude planetary

208 waves.

209

210 **Methods**

211

212 **Observations.** Monthly-mean T_L and P_L from January 1979 to December 2012

213 were taken from the CRUTEM4 and GPCP v2.2 data sets, respectively. CRUTEM4

214 data[27] are derived from in situ observations at meteorological stations. GPCP

215 data[28] are derived from a combination of in situ measurements and satellite

216 estimates. For this study, GPCP data were re-gridded to the CRUTEM4 grid (5° by

217 5° longitude-latitude). The global-mean T_L and P_L have been subtracted from the

218 grid-box values. This procedure removed global-mean variability and trends, but

219 retained regional signatures such as those associated with planetary wave

220 changes.

221 **Extremes.** We derived T_L and P_L anomalies (denoted T_L' and P_L') by removing

222 the relevant climatological monthly mean at each grid-box. Absolute values (i.e.,

223 the modulus) of T_L' and P_L' (denoted $|T_L'|$ and $|P_L'|$) are used to describe the

224   magnitude of the anomalies irrespective of their sign. This is appropriate

225   because planetary waves tend to induce positive T_L (and perhaps P_L) anomalies

226   at some longitudes and negative anomalies at other longitudes. Grid-point

227   anomalies were area-averaged over eight geographical regions: mid-latitudes

228   (ML; 35-60°N, 180°E-180°W), western North America (wNAm; 35-60°N, 115-

229   150°W), central North America (cNAm; 35-60°N, 80-115°W), eastern North

230   America (eNAm; 35-60°N, 45-80°W), Europe (Euro; 35-60°N, 25°E-15°W),

231   western Asia (wAsia; 35-60°N, 25-65°E), central Asia (cAsia; 35-60°N, 65-105°E)

232   and eastern Asia (eAsia; 35-60°N, 105-145°E). These regions (shown in Fig. 3)

233   were chosen *a priori* based on conventional (sub-) continental boundaries and

234   are approximately equal in area and together they cover all the mid-latitude

235   landmasses. The area-averaged monthly time-series were normalised by

236   removing the climatological mean and dividing by the standard deviation for

237   each calendar month. For each region, we then defined "extreme months" as the

238   40 cases (approximately 10%) with largest $|T_L'|$ or $|P_L'|$; and "near-average"

239   months as the 40 cases with smallest $|T_L'|$ or $|P_L'|$. "Hot", "cold", "wet" and "dry"

240   months are defined based on the 40 months with largest T_L', smallest T_L', largest

241   P_L' and smallest P_L', respectively. The selected years are provided in

242   Supplementary Discussion S6.

243   **Wave amplitude.** We analyse amplitudes of planetary waves in the monthly-

244   mean mid-tropospheric mid-latitude circulation, with zonal wave numbers 3-8.

245   Amplitudes were defined based upon Fourier analysis of 500 hPa geopotential

246   heights (Z_{500}), meridionally averaged over mid-latitudes (35-60°N), as a function

247   of longitude. Monthly-mean Z_{500} were taken from the ERA-Interim reanalysis[29].

248   This approach is consistent with the "zonal amplitude" metric used in ref. 18,

249   except here we use monthly-mean Z_{500} averaged over latitudes 35-60°N rather

250   than daily values at 45°N. Whilst multi-decadal trends in planetary-wave

251   amplitude are sensitive to how amplitude is defined[18,20], month-to-month

252   variability of amplitude is highly consistent using the two frameworks outlined

253   in ref. 18. In this manuscript we exclusively consider amplitude variability (not

254   trends) and thus, use only one definition of planetary-wave amplitude.

255   **Statistics.** Differences in sample means were assessed using an unequal variance

256   t-test. This is an adaptation of the Student's t-test that accounts for the two

257   samples having different sizes and possibly unequal variances[30]. Differences in

258   sample variance were assessed using a Fisher f-test. We tested against the null

259   hypothesis that the two sample means or variances are equal. The null

260   hypothesis was rejected if the probability of equal means or variances is less

261   than 10% ($p < 0.1$).

262

263   **References**

264

265   1.   Coumou, D. & Rahmstorf, S. A decade of weather extremes. *Nature Clim.*

266   *Change* **2**, 491-496 (2012).

267   2.   Rahmstorf, S. & Coumou, D. Increase of extreme events in a warming world.

268   *Proc. Natl. Acad. Sci. USA.* **108**, 17905–17909 (2011).

269   3.   Dole, R. *et al*. Was there a basis for anticipating the 2010 Russian heat

270   wave? *Geophys. Res. Lett.* **38**, L06702 (2011).

271   4.   Otto, F. E. L., Massey, N., van Oldenborgh, G. J., Jones, R. G. & Allen, M. R.

272   Reconciling two approaches to attribution of the 2010 Russian heat wave.

273   *Geophys. Res. Lett.* **39**, L04702 (2012).

274   5.   Trenberth, K. E. & Fasullo, J. Climate extremes and climate change: The

275   Russian heat wave and other climate extremes of 2010. *J. Geophys. Res.* **117**,

276   D17103 (2012).

277   6.   Peterson, T. C., Stott, P. A. & Herring, S. Explaining extreme events of 2011

278   from a climate perspective. *Bull. Amer. Meteor. Soc.* **93**, 1041–1067 (2012).

279   7.   Peterson, T. C., Hoerling, M. P., Stott, P. A. & Herring, S. C. Explaining

280   extreme events of 2012 from a climate perspective. *Bull. Amer. Meteor. Soc.*

281   **94**, S1-S74 (2013).

282   8.   Stott, P. A., Stone, D. A. & Allen, M. R. Human contribution to the European

283   heatwave of 2003. *Nature* **432**, 610–614 (2004).

284   9.   Zwiers, F. W., Zhang, X. & Feng, Y. Anthropogenic influence on long return

285   period daily temperature extremes at regional scales. *J. Clim.* **24**, 881–892

286   (2011).

287   10.   Dai, A. Drought under global warming: a review. *WIREs Clim. Change* **2**, 45–

288   65 (2011).

289   11.   Pall, P. et al. Anthropogenic greenhouse gas contribution to flood risk in

290   England and Wales in autumn 2000. *Nature* **470**, 382–385 (2011).

291   12.   Min, S.–K., Zhang, X., Zwiers, F. W. & Hegerl, G. C. Human contribution to

292   more-intense precipitation extremes. *Nature* **470**, 378–381 (2011).

293   13.   Hansen, J., Sato, M. & Ruedy, R. Perception of climate change. *Proc. Natl.*

294   *Acad. Sci. USA* **109**, 14726-14727 (2012).

295   14.   Field, C.B., *et al*. (eds) *Managing the Risks of Extreme Events and Disasters to*

296   *Advance Climate Change Adaptation* (Cambridge Univ. Press, 2012).

297   15.   Francis, J. A. & Vavrus, S. J. Evidence linking Arctic amplification to extreme

298   weather in mid-latitudes. *Geophys. Res. Lett.* **39**, L06801 (2012).

299   16. Liu, J., Curry, J. A., Wang, H., Song, M. & Horton, R. M. Impact of declining

300   Arctic sea ice on winter snowfall. *Proc. Natl. Acad. Sci. USA* **109**, 4074-4079

301   (2012).

302   17. Petoukhov, V., Rahmstorf, S., Petri, S. & Schellnhuber, H. J. Quasiresonant

303   amplification of planetary waves and recent Northern Hemisphere weather

304   extremes. *Proc. Natl. Acad. Sci. USA* **110**, 5336-5341 (2013).

305   18. Screen, J. A. & Simmonds, I. Exploring links between Arctic amplification

306   and mid-latitude weather. *Geophys. Res. Lett.* **40**, 959-964 (2013).

307   19. Screen, J. A. & Simmonds, I. Caution needed when linking weather extremes

308   to amplified planetary waves. *Proc. Natl. Acad. Sci. USA*, **110**, E2327 (2013).

309   20. Barnes, E. A. Revisiting the evidence linking Arctic amplification to extreme

310   weather in midlatitudes. *Geophys. Res. Lett.* **40**, 4728-4733 (2013).

311   21. Leiserowitz, A., Maibach, E., Roser-Renouf, C., Feinberg, G. & Howe, P.

312   *Extreme Weather and Climate Change in the American Mind*. (Yale Univ. &

313   George Mason Univ., 2012).

314   22. Peings, Y. & Magnusdottir, G. Response of the wintertime Northern

315   Hemisphere atmospheric circulation to current and projected sea ice

316   decline: a numerical study with CAM5. *J. Clim.* doi:10.1175/JCLI-D-13-

317   00272.1 (2013).

318   23. Screen, J. A. & Simmonds, I. The central role of diminishing sea ice in recent

319   Arctic temperature amplification. *Nature* **464**, 1334-1337 (2010).

320   24. Serreze, M. C. & Barry, R. G. Processes and impacts of Arctic amplification: A

321   research synthesis. *Global and Planetary Change* **77**, 85-96 (2011).

322   25.   Hoskins, B. J. & Karoly, D. J. The steady linear response of a spherical

323   atmosphere to thermal and orographic forcing. *J. Atmos. Sci.* **38**, 1179-1196

324   (1981).

325   26.   Teng, H., Branstator, G., Wang, H. Meehl, G. A. & Washington, W. M.

326   Probability of US heat waves affected by a subseasonal planetary wave

327   pattern. *Nature Geoscience* doi:10.1038/ngeo1988 (2013).

328   27.   Jones, P. D., *et al.* Hemispheric and large-scale land surface air temperature

329   variations: an extensive revision and an update to 2010. *J. Geophys. Res.*

330   **117**, D05127 (2012).

331   28.   Adler, R. F., *et al.* The version 2 Global Precipitation Climatology Project

332   (GPCP) monthly precipitation analysis (1979-Present). *J. Hydrometeor.* **4**,

333   1147-1167 (2003).

334   29.   Dee, D. P., *et al.* The ERA-Interim reanalysis: configuration and performance

335   of the data assimilation system. *Q. J. R. Meteorol. Soc.* **137**, 553–597 (2011).

336   30.   Moser, B. K. & Stevens, G. R. Homogeneity of variance in the two-sample

337   means test. *Amer. Stat.* **46**, 19–21 (1992).

338

344

Tables

Table 1: Differences in planetary-wave amplitude anomalies between
months of extreme weather and climatology.

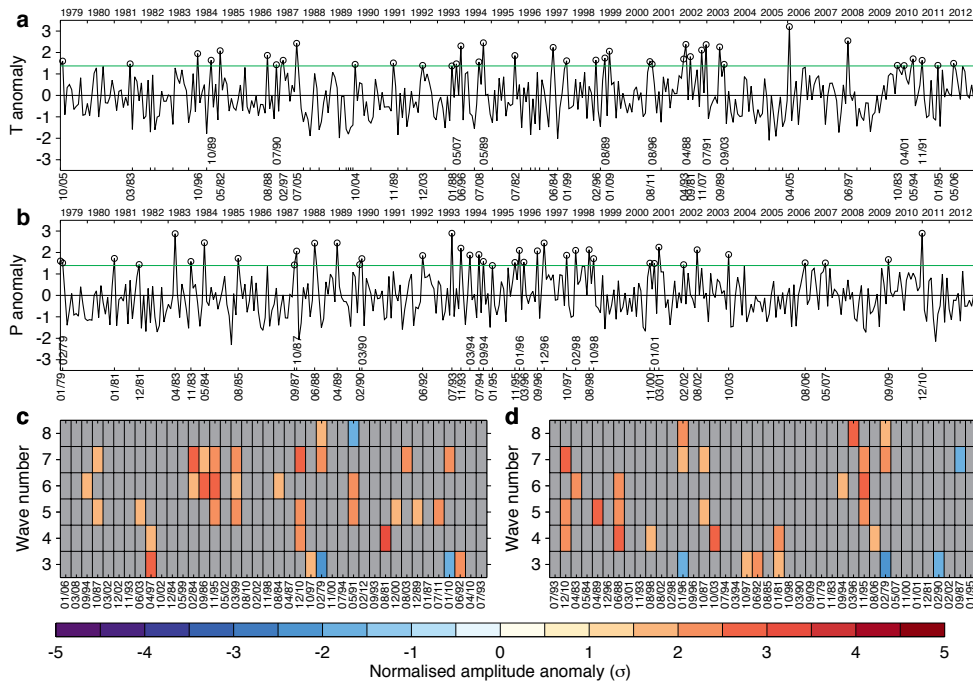|	Hot		Cold		Wet		Dry	
	t	f	t	f	t	f	t	f
wNAm	***2.31***	***1.22***	-0.05	1.13	0.71	1.07	1.05	1.05
cNAm	1.11	***1.19***	1.48	***1.21***	***-1.80***	-1.09	***2.52***	***1.25***
eNAm	-1.18	-1.02	***3.54***	***1.37***	1.08	***1.18***	0.25	1.03
Euro	0.78	1.00	1.15	1.01	0.08	1.02	***2.54***	1.10
wAsia	-0.45	-1.12	0.70	-1.03	***2.45***	1.03	-0.86	-1.01
cAsia	***3.11***	1.02	0.28	1.11	0.25	-1.01	***2.94***	1.11
eAsia	-1.24	-1.12	0.12	1.14	-0.04	***1.21***	-0.05	-1.07

The t and f statistics corresponding to, respectively, differences in mean planetary-wave amplitude and differences in amplitude variance between composites of months with extreme weather and climatology. Statistics are provided separately for four types of weather extreme (hot, cold, wet and dry) and for eight geographical regions. Differences in mean amplitude or variance that are significant at the 90% confidence level are shown in bold italic type. Regions and their abbreviations are shown in Fig. 3.
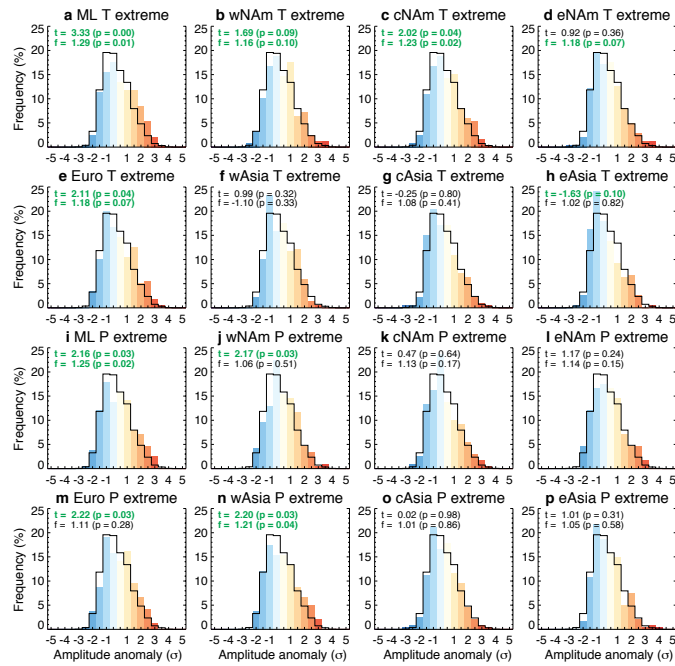
Figure 1: Planetary-wave amplitude anomalies during months of extreme weather. Normalised monthly time-series of mid-latitude- (35-60°N) mean land-based absolute temperature anomalies (**a**) and absolute precipitation anomalies (**b**), 1979-2012. In **a** and **b**, the 40 months with largest values are identified by circles and labelled on the lower x-axis, and the green line shows the threshold value for extremes. Normalised wave amplitude anomalies, for wave numbers 3-8, during 40 months of mid-latitude- mean temperature extremes (**c**) and precipitation extremes (**d**). In **c** and **d**, the months are labelled on the abscissa in order of decreasing extremity from left to right. Grey shading masks anomalies that are not statistically significant at the 90% confidence level; specifically, anomalies with magnitude smaller than 1.64σ, the critical value of a Gaussian (normal) distribution for a two-tailed probability p = 0.1. Red shading indicates wave numbers that are significantly amplified compared to average and blue shading indicates wave numbers that are significantly attenuated compared to average.

a ML T extreme **b** wNAm T extreme **c** cNAm T extreme **d** eNAm T extreme
e Euro T extreme **f** wAsia T extreme **g** cAsia T extreme **h** eAsia T extreme
i ML P extreme **j** wNAm P extreme **k** cNAm P extreme **l** eNAm P extreme
m Euro P extreme **n** wAsia P extreme **o** cAsia P extreme **p** eAsia P extreme

378

Figure 2: Frequency distributions of planetary-wave amplitude anomalies during months of extreme weather. Probability density functions (PDFs) for normalised wave amplitude anomalies (wave numbers 3-8) during 40 months of extreme temperature over eight geographical regions: ML (**a**), wNAm (**b**), cNAm (**c**), eNAm (**d**), Euro (**e**), wAsia (**f**), cAsia (**g**) and eAsia (**h**); and during 40 months of extreme precipitation over the same 8 regions (**i-p**), respectively. The coloured bars show the relative frequency (expressed as a percentage of the total number of anomalies) of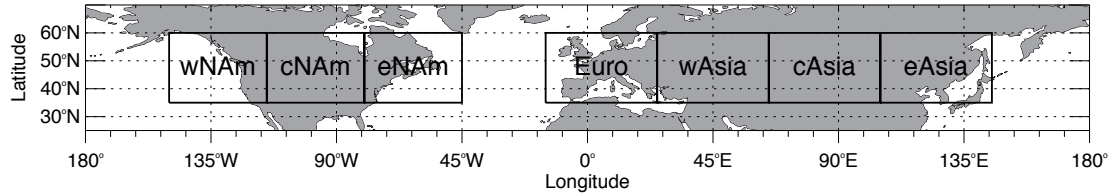 amplitude anomalies in bins of 0.5σ. The black lines show the climatological frequencies. The t and f statistics and their associated p values are provided, with bold green text highlighting values that are statistically significant at the 90% confidence level. The regions and their abbreviations are shown in Fig. 3.
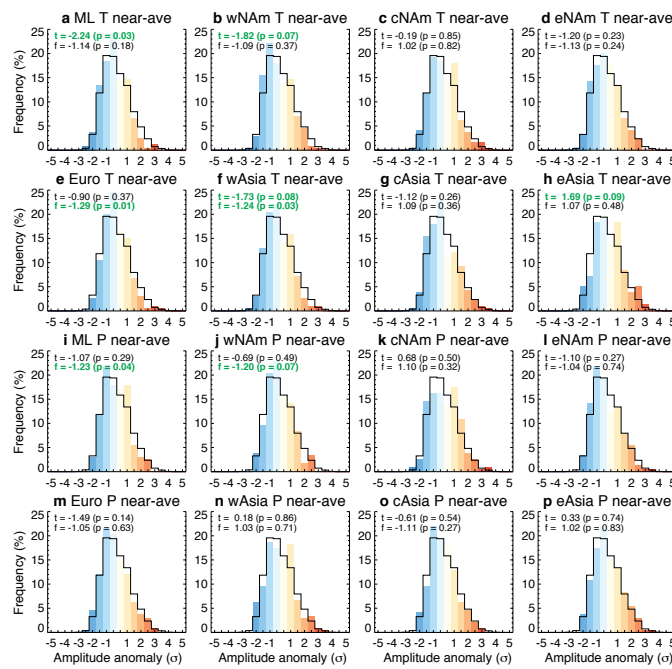
391

Figure 3: The geographical regions used in this study. Black boxes show the regions and are labelled with their abbreviations.

Figure 4: Frequency distributions of planetary-wave amplitude anomalies during months of near-average weather. As Fig. 2, but for months of near-average temperature (**a-h**) and precipitation (**i-p**).